

## Image Planes and Surface States

M. Weinert, S. L. Hulbert, and P. D. Johnson

*Physics Department, Brookhaven National Laboratory, Upton, New York 11973*

(Received 2 August 1985)

We show that the binding energy of surface states is a multibranch function of the image-plane position. The states of the Rydberg series (including the conventional crystal-derived states) have a unique labeling in terms of the number of extrema in the wave function beyond the crystal edge, and the spatial extent of the image states is determined by their binding energy. In addition, we find that the image plane is further from the crystal edge on more loosely packed surfaces and that dynamical corrections to the image potential account for increases in the effective mass of  $< 5\%$ .

PACS numbers: 73.20.Cw

Recently there has appeared in the literature a number of papers<sup>1-4</sup> reporting the observation, with use of the technique of inverse photoemission, of a new class of unoccupied surface states derived from the long-range image potential. The observation of these states, known as image states, has led to a renewed interest in the factors that determine the binding energies of surface states in general. In particular, two models<sup>5,6</sup> have appeared which discuss the influence on the binding energies of these states of, in the first case, the surface-barrier potential running perpendicular to the surface or, in the second case, the surface corrugation potential running parallel to the surface.

The first model,<sup>5</sup> referred to hereafter as the phase analysis model, was originally proposed to account for the binding energies of the Rydberg series of image states.<sup>7</sup> This model treated the states as electron waves undergoing multiple reflections between the infinite crystal barrier on one side and the attractive image potential on the other. Echenique and Pendry<sup>7</sup> had suggested that for discrete cyclic values of the sum of the phase changes on reflection from these two barriers there would exist bound or stationary states. When this model was first confirmed for the image states<sup>5</sup> it became apparent that the same model could be used to make reasonable quantitative predictions of the binding energies of the more conventional crystal-derived or Shockley states.<sup>5,8</sup>

The second or surface corrugation model<sup>6</sup> suggested that the hydrogenic series of states derived from the image potential would deviate from free-electronlike behavior through the perturbation of the surface corrugation potential. Concomitant with the resulting change in the effective masses of the states would be an increase in their binding energies. In particular, for the  $n=1$  Rydberg member this increase would be of the order of a few electronvolts, such that this state would correspond to the crystal-derived or Shockley state.<sup>9</sup> Elsewhere we have demonstrated that this model, which was originally applied to Ag(001), is unlikely and certainly not applicable to Cu(001).<sup>10</sup>

In this Letter we evolve a new model with the

essential physics that allows us to examine both the image-potential-derived and the crystal-derived surface states within a common framework. With this new approach we are able to derive the relationship between these two classes of states. Further, we are able to examine the role of the crystal potential, the image potential, and the surface corrugation in determining the binding energies of the states. Finally, we are able for the first time to label these states unambiguously with the quantum numbers appropriate to mathematical rigor.

Shown schematically in Fig. 1, the model follows the original Goodwin model<sup>11</sup> of surface states in representing the crystal as the inner potential modulated by the appropriate Fourier component of the crystal potential running perpendicular to the surface of interest. However, rather than using the step potential of Goodwin's model we represent the solid-vacuum interface by a plateau region which merges into the long-range image potential defined from an adjustable image plane.

In this interface region, the image potential saturates due to many-body effects and is more repulsive than the bulk potential. As a reasonable approximation, we therefore take the plateau potential equal to the max-

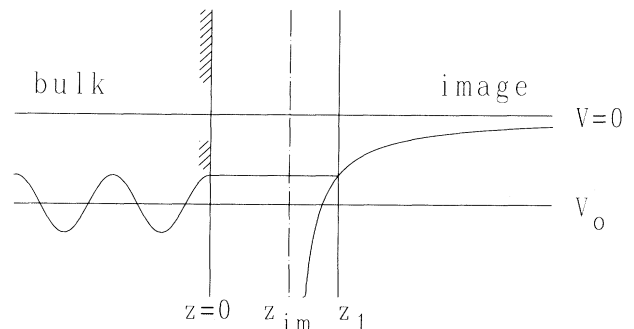


FIG. 1. Schematic representation of the potential used. The bulk potential ( $z < 0$ ) is determined by the reciprocal-lattice vector  $g$ , the width of the gap ( $2V_g$ ), and the position of the vacuum level relative to the gap (midgap is given by  $\hbar^2 g^2 / 8m + V_0$ ). The potential is imagelike for  $z > z_1$ .

imum of the modulated bulk potential. For the systems we have considered this choice of the plateau potential is consistent with both the calculated saturation of the dynamical image potential and the results of more elaborate self-consistent calculations<sup>10</sup> for the potential at the crystal edge.

Inside the crystal, the wave functions for states within the nearly-free-electron band gap are of the form described by Goodwin. In the image region, the Schrödinger equation reduces to the well-known Whittaker equation for the confluent hypergeometric functions. The solutions that are finite at infinity are just the Whittaker functions  $W_{\kappa, 1/2}(x)$ ,  $x = (z - z_{\text{im}})/2\kappa$ , where the parameter  $\kappa$  is related to the binding energy  $\epsilon_b$  by ( $\hbar = m = |e| = 1$ )

$$\epsilon_b = \frac{1}{32\kappa^2} = \frac{0.85 \text{ eV}}{\kappa^2}. \quad (1)$$

Note that the parameter  $\kappa$ , and hence the binding energy of the state, enters both in the order of the Whittaker function and the argument.  $\kappa$  is a continuous parameter ranging between zero and infinity. For integer values of  $\kappa$ , Eq. (1) defines a Rydberg series and the Whittaker functions are proportional to the standard hydrogenic eigenfunctions. In the plateau region, the wave functions are combinations of incoming and outgoing plane waves with wave vectors given by  $\hbar^2 k^2/2m = -V_0 - 2|V_g| - \epsilon_b$ .

We now match logarithmic derivatives,  $L[u] = d \ln u / dz$ , of the wave functions at  $z = 0$  and  $z = z_1$ . If the logarithmic derivative of the Whittaker function at  $z_1$  for a binding energy  $\epsilon_b$  is  $L_1$  and the corresponding log derivative at  $z = 0$  for the crystal (Goodwin) wave function is  $L_0$ , then we obtain an equation for  $z_1$ :

$$\tan k z_1 = k \frac{L_0 - L_1}{k^2 + L_0 L_1}. \quad (2)$$

The quantity  $z_1 - z_{\text{im}}$  is given simply by the requirement that the image potential  $-\frac{1}{4}(z_1 - z_{\text{im}})$  is equal to the plateau potential, which in turn is determined by the work function and the bulk band structure. Hence, Eq. (2) yields the position of the image plane relative to the crystal edge for states within the band gap. Extending the model we can determine similarly the position of the image plane for resonance states whose energies overlap the bulk bands. In Fig. 2 we show the calculated value of  $\kappa$  as a function of the position of the image plane for parameters defining the potential appropriate to Cu(111) and Cu(001).

Our first important observation is that the binding energy, or  $\kappa$ , is a rapidly varying multibranch function of the position of the image plane, corresponding to the branches of the arctangent. If the system is to support a state at the experimentally observed binding energies around  $\kappa \approx 1$  (0.6–0.8 eV), the image plane lies outside of the jellium edge. Furthermore, the image

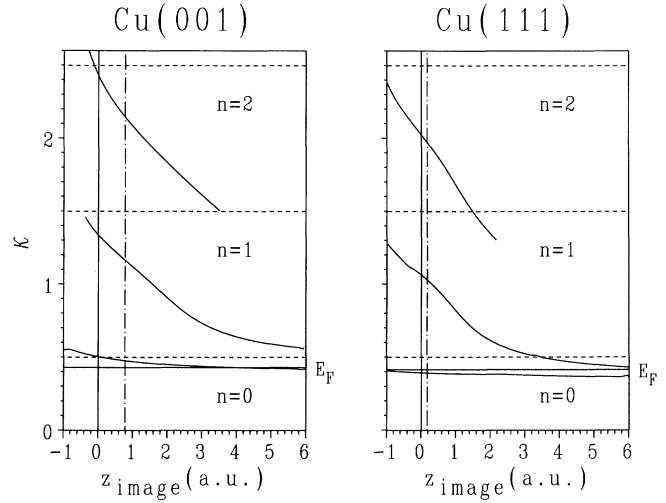


FIG. 2. The binding-energy parameter  $\kappa$  as a function of the image-plane position for Cu(001) and Cu(111). The image plane required to reproduce the experimental  $n = 1$  energy is marked by the dashed line.

plane for the more loosely packed Cu(001) surface is farther out compared to the Cu(111) surface (see Table I), i.e., in the terminology of Lang and Kohn,<sup>12</sup> the centroid of the induced screening charge is further from the jellium edge for loosely packed surfaces.

Given the position of the image plane deduced from fitting the experimental binding energy of the states near  $\kappa \approx 1$ , our model has no arbitrary adjustable parameters. We predict states to exist for every branch at energies corresponding to this single image plane. In Table I, we give the image-plane positions for a few of the surfaces that we have considered, as well as the corresponding energies of the states corresponding to the first three branches.

A significant result of these calculations is that in all cases there exists either a surface state or resonance for  $\kappa \leq \frac{1}{2}$ . For Cu(111) and Ag(111), these states reproduce the experimental binding energies<sup>13,14</sup> of the observed surface states around  $\Gamma$ ; on the (001) surfaces of Cu and Ag, they are resonances which have been observed in inverse photoemission.<sup>10,15</sup> These states are of the conventional “crystal-derived” type, i.e., their existence, as we show below, does not depend on the long-range nature of the image potential.

In analogy with atomic physics, one can define a quantum-defect parameter  $\alpha$  such that  $\kappa = n + \alpha$ ,  $|\alpha| \leq \frac{1}{2}$ . Then for a given  $\kappa$ , the “principal” quantum number  $n$  is uniquely defined. From Fig. 2, we see that each branch of the image-plane position corresponds to a range in  $\kappa$  of  $\approx 1$ . In addition to this being the natural physical labeling of the states, it is also the natural mathematical labeling, i.e., our labeling is

TABLE I. Position of the image plane (in atomic units) that places the  $n = 1$  state as given. The corresponding  $n = 0, 2$  levels ( $n = 0$  relative to the Fermi level,  $n = 1, 2$  relative to the vacuum level; energies in electronvolts) and experimental results (in parentheses) are also given. Resonances are marked by asterisks.

	$z_{\text{im}}$	$n = 0$	$n = 1$	$n = 2$
Cu(001)	0.77	0.85* ( $\approx 1.0$ ) <sup>a,b</sup>	0.62 (0.64) <sup>a,b,c</sup>	0.18
Cu(111)	0.17	-0.58 (-0.39) <sup>d</sup>	0.80 (0.83) <sup>e</sup>	0.22*
Ag(100)	0.71	1.22* (1.0) <sup>f</sup>	0.62 (0.6) <sup>f</sup>	0.19
Ag(111)	0.21	0.04 (-0.12) <sup>e</sup>	0.77 (0.77) <sup>e</sup>	0.22* (0.23) <sup>e</sup>

<sup>a</sup>Reference 10.

<sup>b</sup>Reference 15.

<sup>c</sup>Reference 5.

<sup>d</sup>Reference 13.

<sup>e</sup>Reference 14.

<sup>f</sup>Reference 6.

arbitrary only to the extent that the labeling of the hydrogenic levels and the Whittaker functions is arbitrary. To make this discussion more rigorous, we proceed by deriving a new expansion of the Whittaker functions about the hydrogenic solutions in powers of the quantum-defect parameter. To first order in  $\alpha$ , the Whittaker functions for  $n = 0, 1, 2$  ( $|\alpha| \leq \frac{1}{2}$ ) are

$$\begin{aligned}
 W_{\alpha, 1/2}(x) &= e^{-1/2x} \left\{ 1 - \alpha \left[ (e^x - 1) \ln x - \sum_{m=0}^{\infty} \frac{x^m}{m!} \psi(m+1) \right] + \dots \right\}, \\
 W_{1+\alpha, 1/2}(x) &= x e^{-1/2x} \{ 1 - \alpha(1/x - \ln x) + \dots \}, \\
 W_{2+\alpha, 1/2}(x) &= e^{-1/2x} \{ (x-2) - \alpha[3 + (2-x) \ln x - 1/x] + \dots \},
 \end{aligned} \tag{3}$$

where  $\psi(z) = d \ln \Gamma(z)/dz$ . The zeroth-order terms for  $n = 1, 2, \dots$  are just proportional to the standard hydrogenic orbitals as can be seen by writing  $x = 2Zr/n$ ; for the image potential, the "nuclear" charge is  $Z = \frac{1}{4}$ .

The  $n = 0$  state is not allowed in the atomic case because the wave function diverges as  $x^{-1}$  for small  $x$ . For the surface, however, the image potential saturates and this solution is allowed. The leading term of the  $n = 0$  state is a decaying exponential,  $\exp[-(2\epsilon_b)^{1/2}]$ , identical to the solution for a step potential.<sup>11</sup> Hence, we have demonstrated that the  $n = 0$  state of the image potential (e.g., Fig. 3) corresponds to the Shockley or surface state. Moreover, we conclude on quite general grounds that all surface-barrier potentials ranging between the limiting cases of the image and the step potentials can support a surface state or resonance with wave functions represented by an exponentially decaying function outside the crystal. Conversely, the  $n = 0$  state is not particularly affected by the large  $z$  behavior of the potential and hence we would expect (and indeed find in the calculations) that the  $n = 0$  states are tied to the Fermi level. As seen in Fig. 3, the image states for  $n \geq 1$  have maxima in their densities outside of the crystal; typically  $\approx 90\%$  of their density is beyond the crystal edge. These states are therefore

not strongly affected by shifts of the bulk potential, i.e., changes in the work function, and hence they should follow the vacuum level.

An important consequence of this discussion con-

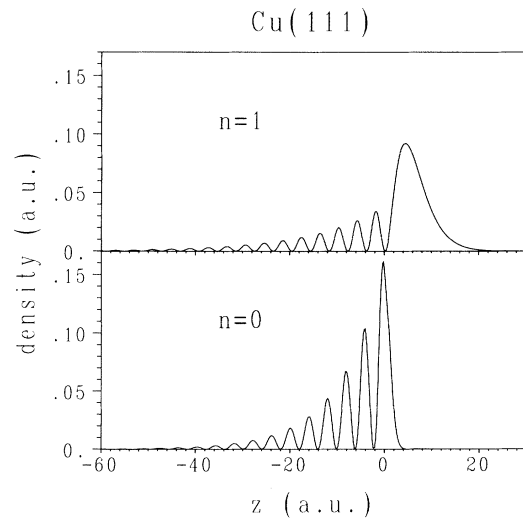


FIG. 3. Density of the  $n = 0$  surface state and  $n = 1$  image state for Cu(111).

cerns the effect of corrugation of the surface potential on the energy position of the  $n=1$  state. Our results unambiguously demonstrate that in situations where a perturbation treatment of the corrugation is justified, the spatial extent of the image states depends only on their binding energy, or equivalently, the parameter  $\kappa$ . We conclude that the  $n=1$  states are observed at a binding energy of  $\approx 0.6$  eV on the (001) surfaces of Ag and Cu and have a maximum  $\approx 2$  Å beyond the crystal edge and not, as claimed in Ref. 6, at  $\approx 12$  Å. These conclusions are in agreement with the results from variational calculations that the effect of the corrugation of the potential on the binding energies and effective masses is small for real surfaces.<sup>10, 16</sup>

Finally, we examine the role of a dynamic image potential on the effective mass. The classical image potential applies to a static charge outside of the metal surface. For electrons with finite velocity, the dynamical potential saturates because the surface modes (the plasmons) which give rise to the image potential are unable to adjust rapidly enough. We apply a semiclassical approximation<sup>17</sup> to determine the self-consistent dynamical potential for parameters typical of the situation encountered in inverse-photoemission experiments. The effective potential saturates in a manner that results in a single-particle potential much like the one used in our model. Applying perturbation theory, we find that the dynamical potential increases the effective mass, but this effect is  $\leq 5\%$  for the  $n=1$  state and an order of magnitude less for the  $n=2$  state. Therefore, using realistic parameters, we conclude that large effective masses ( $\approx 1.3$ – $1.5$ )<sup>6</sup> for the image states cannot be explained either by the corrugation of the single-particle potential or by simple many-body dynamical corrections to the image potential.

Our results clearly support the conclusions of the phase analysis model (which with further approximations can be derived from our model) over that of the surface corrugation model. However, we also note that for the first time we have clearly shown why the phase analysis method should be capable of providing quantitative predictions of the binding energies of the crystal-derived states. We are able to determine the relationship between the crystal-derived and the image-derived states. More importantly, we have been able to demonstrate the dependence of the binding energies of these states on the position of the image plane, which we determine to be further out on more

loosely packed surfaces. We find that the binding energy of the states is a rapidly varying multibranch function of the image-plane position and this results in a Rydberg series of levels. Contrary to the belief that the labeling of these states is semantics we find that the states of this series have a unique labeling determined by the number of extrema in the wave functions beyond the crystal or jellium edge. While all surface potentials can support the  $n=0$  crystal-derived (Shockley) states, the existence of the higher members with  $n \geq 1$  depends on the long-range nature of the image potential.

Work performed at Brookhaven National Laboratory is supported by the Division of Materials Sciences, U.S. Department of Energy, under Contract No. DE-AC02-76CH00016.

<sup>1</sup>P. D. Johnson and N. V. Smith, Phys. Rev. B **27**, 2527 (1983).

<sup>2</sup>V. Dose, W. Altman, A. Goldman, U. Kolac, and J. Rogozik, Phys. Rev. Lett. **52**, 1919 (1984).

<sup>3</sup>D. Straub and F. J. Himpsel, Phys. Rev. Lett. **52**, 1922 (1984).

<sup>4</sup>B. Reihl, K. H. Frank, and R. R. Schlittler, Phys. Rev. B **30**, 7328 (1984).

<sup>5</sup>S. L. Hulbert, P. D. Johnson, N. G. Stoffel, W. A. Royer, and N. V. Smith, Phys. Rev. B **31**, 6815 (1985).

<sup>6</sup>N. Garcia, B. Reihl, K. H. Frank, and A. R. Williams, Phys. Rev. Lett. **54**, 591 (1985).

<sup>7</sup>P. M. Echenique and J. B. Pendry, J. Phys. C **11**, 2065 (1978).

<sup>8</sup>N. V. Smith, to be published.

<sup>9</sup>B. Reihl, in Proceedings of the Seventh European Conference on Surface Science, Aix-en Provence, France, 1–4 April 1985, Surf. Sci. (to be published).

<sup>10</sup>S. L. Hulbert, P. D. Johnson, M. Weinert, and R. F. Garrett, to be published.

<sup>11</sup>E. T. Goodwin, Proc. Cambridge Philos. Soc. **35**, 205 (1939).

<sup>12</sup>N. D. Lang and W. Kohn, Phys. Rev. B **1**, 873 (1979).

<sup>13</sup>S. D. Kevan, Phys. Rev. Lett. **50**, 526 (1983).

<sup>14</sup>K. Giesen, F. Hage, F. J. Himpsel, H. J. Riess, and W. Steinman, Phys. Rev. Lett. **55**, 300 (1985).

<sup>15</sup>D. P. Woodruff, S. L. Hulbert, P. D. Johnson, and N. V. Smith, Phys. Rev. B **31**, 4046 (1985).

<sup>16</sup>M. Weinert, Bull. Am. Phys. Soc. **30**, 409 (1985), and unpublished.

<sup>17</sup>R. Ray and G. D. Mahan, Phys. Lett. **42A**, 301 (1972).